Journal of Biomolecular NMR, 5 (1995) 433–437
ESCOM

J-Bio NMR 290

Refocusing revisited: An optimized, gradient-enhanced refocused HSQC and its applications in 2D and 3D NMR and in deuterium exchange experiments

Jonathan H. Davis

Graduate Group in Biophysics, University of California, UCSF box 0448, San Francisco, CA 94143-0448, U.S.A.

Received 21 March 1995
Accepted 8 May 1995

Keywords: ^{15}N-edited NOESY-HSQC; Protein folding; Heteronuclear NMR; Semi-constant time; α-Lytic protease

Summary

2D ^{15}N-^{1}H correlation spectra are ideal for measuring backbone amide populations to determine amide exchange protection factors in studies of protein folding or other structural features. Most protein NMR spectroscopists use HSQC, which has been shown to be generally superior to HMQC in both resolution and sensitivity. The refocused HSQC experiment is intrinsically less sensitive than the regular HSQC, due to T_2 relaxation during the refocusing delays. However, we show here that, when high ^{15}N resolution is needed, an optimized refocused HSQC sequence that utilizes a semi-constant time evolution period and pulsed field gradients has better signal-to-noise ratio and resolution, and integrates more accurately, than a similar HSQC. The differences are demonstrated on a 20 kDa protein. The technique can also be applied to 3D NOESY experiments to eliminate strong NH_2 geminal peaks and their truncation artefacts at a modest cost in sensitivity.

Two-dimensional amide ^{1}H-^{15}N heteronuclear correlation spectra, such as HMQC (Müller, 1979) and HSQC (Morris and Freeman, 1979), in theory contain one peak for each backbone amide. Since the ^{1}H-^{15}N coupling constant is independent of secondary or tertiary structure, the intensities of the peaks display only minor variation (in the absence of some broadening mechanism), and such spectra are commonly used to determine amide exchange rates and to observe the protection factors of amides at various stages of folding (Gooley et al., 1992; Mau et al., 1992). The large coupling constant and wide chemical shift dispersion of backbone ^{15}N amides combine to allow correlation experiments to be very sensitive and well resolved, and therefore of greater utility in these applications than homonuclear H^N-H^α correlation experiments. In this communication we present an optimized, semi-constant time, gradient- and resolution-enhanced refocused HSQC (refHSQC) that has better resolution and greater signal-to-noise ratio than a gradient- and resolution-enhanced HSQC without refocusing.

The refocused HSQC was first described by Burum and Ernst (1980), and in its 2D inverse-detected form has been evaluated against other sequences (Bax et al., 1990). It is well known that additional signal loss occurs (when compared with a regular HSQC) due to T_2 relaxation during the refocusing delay, but that by maintaining in-phase heteronuclear single-quantum coherence with decoupling on the protons, the decay during the evolution time is dominated only by dipolar and CSA interactions involving the heteronucleus. During the evolution delay in an HSQC (but not a refHSQC), when the heteronucleus is antiphase with respect to the proton, its relaxation rate is increased by other mechanisms, including proton spin-lattice relaxation and cross-relaxation (Peng et al., 1991). Bax et al. (1990) showed that this leads to broader lines in the HSQC spectrum compared to its refocused counterpart, with both being superior to HMQC. However, with the pulse sequences compared by Bax et al. (1990), it appears that refocusing results in a slightly lower signal-to-noise ratio.

Imperfections in the three additional hard 180° pulses in the refocused version add to its sensitivity loss. We use an improved refocusing scheme (Van Doren et al., 1993; Farmer II, B.T., personal communication) that removes two of these additional pulses, and we also incorporate a semi-constant (or shared time) evolution period (Grzesiek

0925-2738/$ 6.00 + 1.00 © 1995 ESCOM Science Publishers B.V.

and Bax, 1993a; Logan et al., 1993) for the heteronucleus, which for ^{15}N includes about 10 ms of defocusing and refocusing time in the final evolution time. Our comparison is between the refHSQC diagrammed in Fig. 1 (starting at **A**) and a regular gradient- and sensitivity-enhanced (Palmer et al., 1991) HSQC, which is identical except that the semi-constant time period is replaced by the sequence fragment shown in curly brackets in the figure (this sequence is very similar to that given by Kay et al. (1992)). Since Kay et al. demonstrated the superiority of their gradient-enhanced HSQC over other sequences, we compare ours only to their experiment. The sequence presented here contains the same number of pulses (excluding the t_1 decoupling and trim pulses), and provides higher resolution and signal-to-noise ratio when applied to a large (20 kDa) protein. It is important to note that the advantages are maximized when a long acquisition time is used in t_1 (several hundred ms). If a fast experiment is desired, at the expense of resolution in the ^{15}N dimension, then the lines are broad in both experiments, and the refHSQC becomes less sensitive than the HSQC.

Three-dimensional heteronuclear NMR experiments are now becoming routine for assigning and determining the structure of proteins in the 10 to 25 kDa range, with the potential for even larger proteins (Wagner, 1993; Clore and Gronenborn, 1994). The first of these experiments, NOESY-HMQC (Marion et al., 1989a; Zuiderweg and Fesik, 1989), is still in use today. We have found that replacing the HMQC with an enhanced HSQC improves the experiment, but does not fully address the difficulty encountered in the crowded regions where most of the side-chain NH_2 groups are found; while the enhancement scheme reduces the intensity of the side-chain cross peaks by a factor of about two, they are still quite substantial. It can be difficult to distinguish NOESY peaks involving a side-chain amide from those involving a backbone amide that happens to fall in the same region. In addition, due to their long T_2, NH_2 peaks are sharp, and prone to truncation artefacts that propagate through other portions of the spectrum. Since backbone amide-to-amide NOESY peaks are of particular importance in sequential assignment and secondary structure determination, the removal of the large NH_2 geminal cross peaks, and their truncation artefacts, allows a sequential amide cross peak at the same location to be seen (or, alternatively, confirmed to be missing). A well-known property

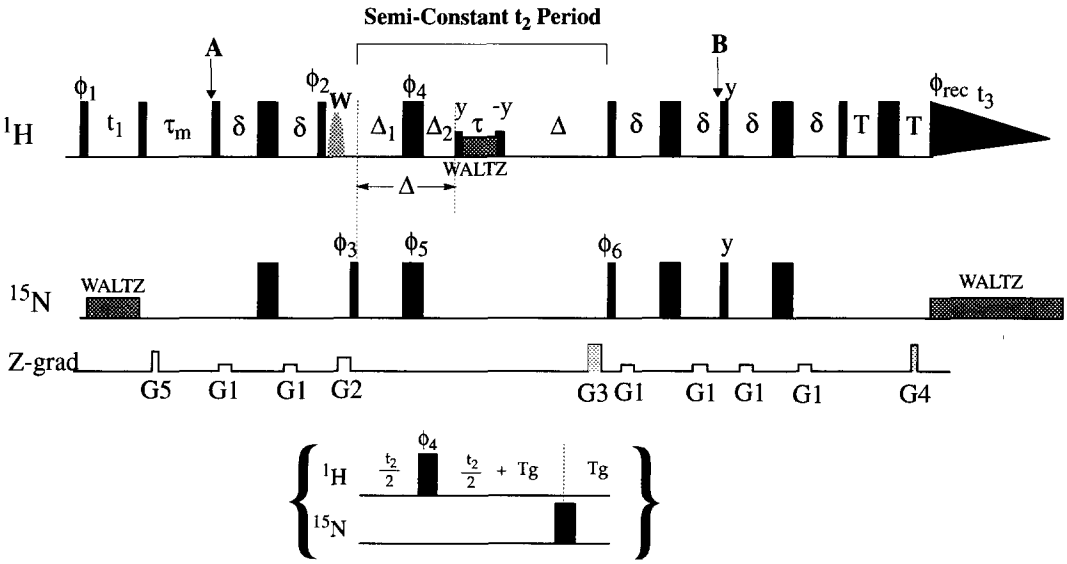

Fig. 1. NOESY-refHSQC pulse sequence: resolution-enhanced 3D sequence that uses a refocused HSQC instead of HMQC for the ^{15}N dimension. Semi-constant time is used in t_2 (Grzesiek and Bax, 1993a; Logan et al., 1993). All unmarked pulses have phase x, and other phases are: ϕ_1 = x,–x; ϕ_2 = y,y,–y,–y; ϕ_3 = x; ϕ_4 = 4(x),4(–x); ϕ_5 = 8(x),8(–x); ϕ_6 = x; and ϕ_{rec} = x,–x,–x,x. ϕ_1 and ϕ_{rec} are incremented in the normal States-TPPI manner for quadrature detection in t_1. For t_2, in each alternate FID, ϕ_6 is incremented by 180° and the sign of G_4 is inverted, and in each alternate t_2 increment, ϕ_3 and ϕ_{rec} are incremented by 180°. The gradients G_3 and G_4 are both about 30 G/cm, and their lengths are 1.2 ms and 125 ms, respectively. The strength of G_4 is adjusted for optimum signal. The data must be presorted before processing (Kay et al., 1992). $\delta \leq \sim 1/4J_{NH}$, or 2.25 ms. $\Delta = 1/2J_{NH}$ = 5.4 ms; T = 500 ms. Delays for the semi-constant time period are calculated as follows: $\Delta_2 = \Delta * (t_2/t_2max)$; $\Delta_1 = \Delta - \Delta_2$; and $\tau = t_2 - (2 * \Delta_2)$. To acquire a 2D correlation spectrum, the sequence begins at point **A**. A water flip-back pulse can be installed as a low-power shaped pulse, phase –x (or ϕ_1 in the case of a 3D experiment), immediately after the ϕ_2 pulse (marked **W** in the sequence; Grzesiek and Bax, 1993b). The trim pulses bordering the proton decoupling period are necessary to maintain maximum effectiveness of the **W** pulse (Kay et al., 1994). If gradients are not available, acquisition is started at point **B**, and ϕ_6 remains x while ϕ_3 and ϕ_{rec} are cycled in the usual States-TPPI manner (Marion et al., 1989b). In this case, water suppression can be achieved without the use of presaturation by installing an x spin-lock pulse on protons just before the ϕ_2 pulse (Messerle et al., 1989). Changes in sample temperature with increasing evolution decoupling time are prevented by installing ^{15}N and ^{1}H pulses at decoupling power before the relaxation delay, with varying durations that complement the evolution time, such that at every increment the total pulse time is constant (Wang and Bax, 1993). The sequence fragment shown at the bottom in curly brackets was used in place of the semi-constant t_2 period when running a regular HSQC for comparison. T_g = 1.375 ms.

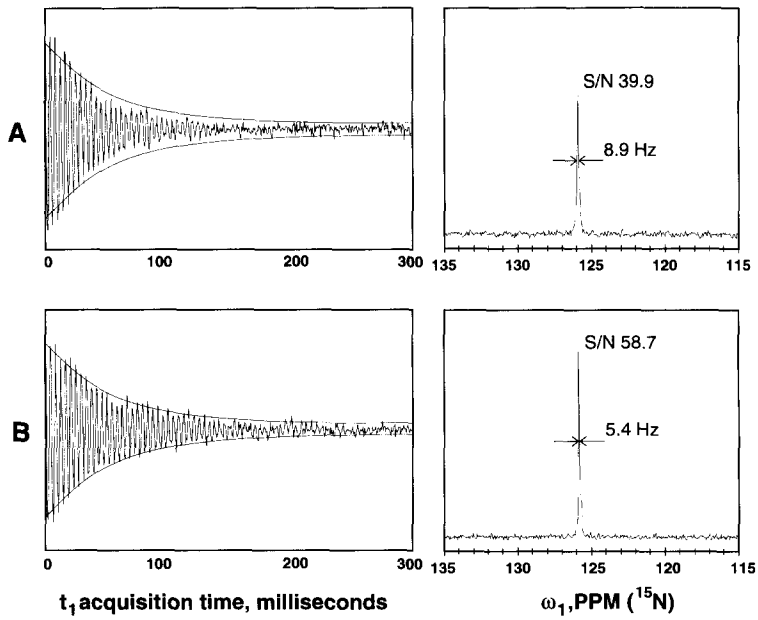

Fig. 2. Comparison of HSQC and refHSQC: t_1 interferogram and ω_1 spectrum of the slice through Val^4 of α-lytic protease, from 2D HSQC (A) and refHSQC (B) spectra collected on a single sample with identical conditions and parameters, on a 600 MHz spectrometer. The transformations were performed without zero-filling or apodization. The envelope of the refHSQC is approximated by the lines drawn on the interferogram; the exact same lines were placed over the HSQC interferogram to highlight the differences in decay properties. Note that in (A) the signal begins slightly higher, but decays much more rapidly, leading to the broader line. All vertical axes are matched between A and B. Spectral widths were 8600 Hz (t_2) and 1700 Hz (t_1), for a final acquisition time in t_1 of 300 ms. Eight scans per FID were acquired, and protons were decoupled using a 3333 Hz field. High-power field strengths were 29 000 Hz for ^1H and 5000 Hz for ^{15}N.

of refocusing is that by tuning the delay, one can choose to maximize or minimize various spin systems, particularly selecting for XH and against XH_2 (Burum and Ernst, 1980). We show here that editing a NOESY with our refHSQC reduces the sensitivity only moderately, while taking advantage of the fact that refocusing edits out NH_2 groups almost entirely, cleaning up those portions of the spectrum where the NH_2 resonances appear. This can be very helpful with proteins containing many asparagine or glutamine residues (α-lytic protease contains 22 of them).

Figure 1 shows the NOESY-refHSQC pulse scheme with gradients and sensitivity enhancement. The INEPT transfer begins at point **A**, and after the ϕ_2 and ϕ_3 pulses the transverse ^{15}N magnetization is antiphase to the protons. Two simultaneous processes occur during the semi-constant t_2 period: ^{15}N refocusing, followed by defocusing to antiphase; and ^{15}N evolution. The refocusing takes place during $\Delta_1+\Delta_2 (= 1/2J_{HN} = \Delta)$. At the end of $\Delta_1+\Delta_2$, ^{15}N is independent of the state of ^1H, so proton decoupling and trim pulses can be applied. During the subsequent Δ period, ^{15}N evolves back to antiphase with respect to ^1H. Meanwhile, the chemical shift evolves in one direction for the time Δ_1, and in the opposite direction for the time $\Delta_2+\Delta+\tau$, so the function for the evolution time is $t_2=\Delta_2+\Delta+\tau-\Delta_1$ (or $2\Delta_2+\tau$). At $t_2=0$ (first slice), $\Delta_1=\Delta$ and $\Delta_2=\tau=0$, and the maximum signal is observed. The remainder of the sequence is the reverse of the beginning (up until **B**), followed by a series of pulses to enhance sensitivity (Palmer et al., 1991; Kay et al., 1992). The semi-constant time period takes advantage of the two Δ delays, which add up to more than 10 ms, and incorporates them into the evolution time. Thus, although the first slice is reduced in intensity due to T_2 relaxation during 2Δ, by the last slice the entire 2Δ period is part of the evolution time. This effectively decreases the rate of decay of the signal envelope in the indirect ^{15}N dimension, resulting in narrower lines. Further narrowing is effected by the fact that in-phase ^{15}N magnetization has longer intrinsic T_2 times than does antiphase magnetization (see above).

The advantage of refocusing is shown in Fig. 2, which displays the t_1 interferogram, from a 2D experiment, of a cross peak that has a unique ^1H chemical shift and is otherwise representative. The envelope of the refHSQC signal is sketched in, and the same lines are drawn over the HSQC signal for ease of comparison. The decay envelopes of the two experiments are clearly different, with the refocused version having a slower decay. A total of 512 complex t_1 points were collected on the same sample with identical instrument settings, and were Fourier transformed with no apodization or zero-filling for a final resolution of 3.34 Hz/point. The line width of the refocused peak is about 40% less, and its signal-to-noise ratio is 47% higher. Zero-filling twice prior to transformation without apodization reduced all line widths by

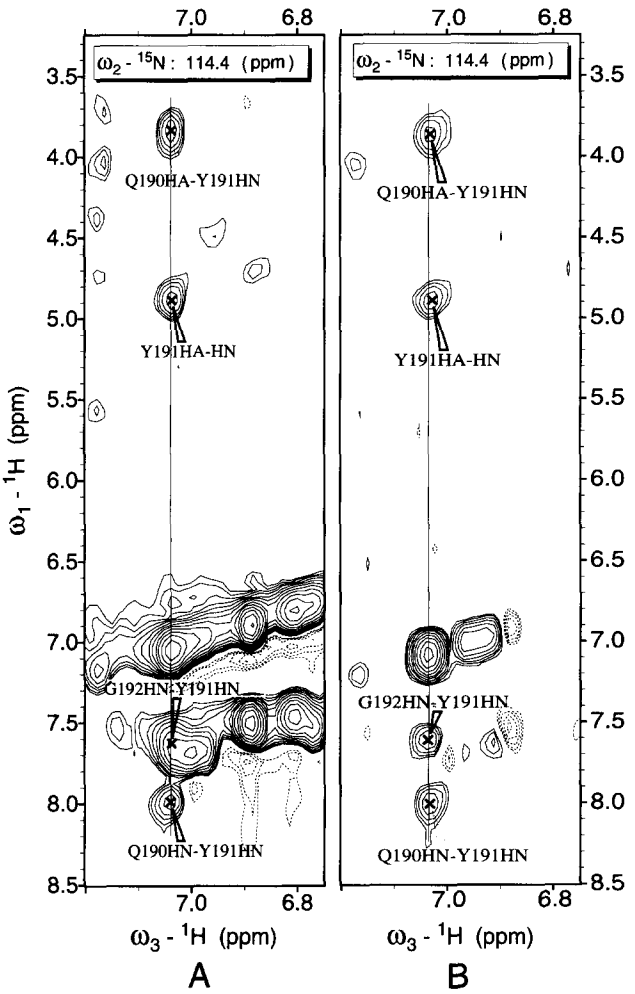

Fig. 3. Slices of 3D NOESY spectra of α-lytic protease showing amide and H^{α} NOEs to Tyr^{191} HN. (A) The NOESY-HSQC experiment, with two sequential amide cross peaks and two H^{α} cross peaks. The cross peak to H^{N} of Gly^{192} is badly overlapped by the geminal cross peak from an unassigned side-chain NH_2 group. (B) The NOESY-refHSQC spectrum of the same region. All the same backbone cross peaks are represented, but here both sequential amide cross peaks are well resolved. Peaks in the refocused spectrum were weaker than those in the HSQC. We measured the loss of signal by comparing the signal-to-noise ratios of 19 randomly chosen resolved cross peaks. We then calculated the ratio of the signal-to-noise ratios (HSQC : refHSQC), which ranged from 1.1 to 1.6 and averaged 1.32. Thus, an average 25% reduction in sensitivity was present in the refocused experiment. Parameters were similar to those described in Fig. 2, with the following changes: four scans were collected per FID, and the spectral widths and number of complex points in the indirect dimensions were 6840 Hz and 58 points for t_1 (proton), and 2000 Hz and 64 points for t_2. The mixing time was 140 ms. Linear prediction of 64 points was used in each indirect dimension, and the final size after zero-filling once in t_1 was $256 \times 128 \times 1024$ points. Apodization consisted of sine-squared functions shifted 80° in t_1 and t_2, and a Lorentzian-to-Gaussian function in t_3.

about 10%, but did not substantially change our results. Application of various apodization functions improved the signal-to-noise ratio up to 50% while increasing line widths proportionally, without substantially changing the ratio between the two spectra (data not shown). Improvements in resolution and signal-to-noise ratio remained through all reasonable processing schemes, and were present throughout the spectrum.

Experiments that measure amide exchange, such as protection factor and Baldwin–Roder-type refolding experiments (Roder et al., 1988; Udgaonkar and Baldwin, 1988), rely on the ability to quantify the percentage of the amides that are protonated. To evaluate the ability of the various 2D sequences to accurately report the concentration of protonated backbone amides, we prepared two test samples of α-lytic protease (20 kDa) in D_2O, with concentrations of 1.5 mM and 0.5 mM. Comparison of the integrated volumes of the peaks should result in a consistent ratio close to 3:1. We ran the best gradient-enhanced and optimized HSQC experiment (Kay et al., 1992) on both samples, and compared it with our 2D refocused HSQC. All spectra used water flip-back, and had a ^1H spectral width of 8600 Hz, 1024 complex points, and were zero-filled once in the proton dimension, and a ^{15}N spectral width of 1700 Hz, 512 complex points, and zero-filling twice in the nitrogen dimension, for a final size (untrimmed) of $2K \times 2K$ points. Apodization consisted of a moderate Lorentzian-to-Gaussian window function. Integrations were performed by Sparky*, our in-house NMR analysis program, which fits a Gaussian in two dimensions and integrates the fitted peak. The ratios between the peak volumes were then taken, and the average and standard deviation were calculated. The average ratio of the HSQC spectra was 2.90, $\sigma = 0.20$, and for refHSQC the average ratio was 2.95, $\sigma = 0.22$. We performed a Student's T test on the distributions, which gave a better than 98% probability that the difference in means was significant ($A(t|\nu) = 0.012$). Since the refHSQC also has a better signal-to-noise ratio and resolution, we feel that it will be a useful experiment in amide exchange experiments, whenever resolution needs to be maximized and speed is not essential (as when exchange has been quenched before NMR measurements).

The 3D NOESY-refHSQC experiment is created by preceding the 2D sequence with a proton evolution time and a NOESY mixing period (Fig. 1, before point **A**). Because this results in a 3D experiment, it is impractical to acquire enough points in ^{15}N to achieve line widths of 5 Hz. However, the semi-constant time feature reduces the decay rate of the signal in the ^{15}N dimension. The use of semi-constant time in NOESY experiments has been associated with artefacts that appear offset in the ^{15}N dimension (Farmer and Mueller, 1994), but while these were present in our spectrum, the only significant ones were echoes of the diagonal peaks, and so also appeared on the proton diagonal. The signal-to-noise ratio of the 3D experiment is reduced by 25% compared to a 3D

*For software availability, please contact I.D. Kuntz, UCSF Box 0446, San Francisco, CA 94143-0446, U.S.A.

NOESY-HSQC, but the editing feature of refocusing eliminates unwanted strong geminal side-chain amide peaks, allowing the detection of important sequential backbone amide–amide peaks that may be in the same region of the spectrum. Figure 3 displays the same slice of two 3D NOESY spectra, centered on a backbone amide that is in the middle of one of the dense groups of side-chain NH_2 signals. In the NOESY-refHSQC the strong side-chain cross peak is eliminated, and the spectrum can be more easily interpreted. While it would not replace the other experiments, we feel that this 3D sequence could be of use as an additional tool for investigations of proteins that display severe overlap with side-chain NH_2 signals.

Acknowledgements

The author would like to thank Sandy Farmer, Dennis Benjamin and Daina Avizonis for helpful discussions and careful reading of the manuscript, Julie Sohl and Don Kneller for help with integrations and statistics, and Vladimir Basus and David Agard for their teaching and guidance. Lewis Kay kindly provided the code for the HSQC experiment. This work was funded through the Howard Hughes Medical Institute, which supports my advisor, David A. Agard, and by NIH training Grant 2 T32 GM08284 and a UCSF REAC grant to David Agard and Vladimir Basus.

References

Bax, A., Ikura, M., Kay, L.E., Torchia, D.A. and Tschudin, R. (1990) *J. Magn. Reson.*, **86**, 304–318.

Burum, D.P. and Ernst, R.R. (1980) *J. Magn. Reson.*, **39**, 163–168.

Clore, G.M. and Gronenborn, A.M. (1994) *Protein Sci.*, **3**, 372–390.

Farmer II, B.T. and Mueller, L. (1994) *J. Biomol. NMR*, **4**, 673–687.

Gooley, P.R., Caffrey, M.S., Cusanovich, M.A. and MacKenzie, N.E. (1992) *Biochemistry*, **31**, 443–450.

Grzesiek, S. and Bax, A. (1993a) *J. Biomol. NMR*, **3**, 185–204.

Grzesiek, S. and Bax, A. (1993b) *J. Am. Chem. Soc.*, **115**, 12593–12594.

Kay, L.E., Keifer, P. and Saarinen, T. (1992) *J. Am. Chem. Soc.*, **114**, 10663–10665.

Kay, L.E., Guang, Y.X. and Yamazaki, T. (1994) *J. Magn. Reson.*, **A109**, 129–133.

Logan, T.M., Olejniczak, E.T., Xu, R.X. and Fesik, S.W. (1993) *J. Biomol. NMR*, **3**, 225–231.

Marion, D., Kay, L.E., Sparks, S.W., Torchia, D.A. and Bax, A. (1989a) *J. Am. Chem. Soc.*, **111**, 1515–1517.

Marion, D., Ikura, M., Tschudin, R. and Bax, A. (1989b) *J. Magn. Reson.*, **85**, 393–399.

Mau, T., Baleja, J.D. and Wagner, G. (1992) *Protein Sci.*, **1**, 1403–1412.

Messerle, B.A., Wider, G., Otting, G., Weber, C. and Wüthrich, K. (1989) *J. Magn. Reson.*, **85**, 608–613.

Morris, G.A. and Freeman, R.J. (1979) *J. Am. Chem. Soc.*, **101**, 760–762.

Müller, L. (1979) *J. Am. Chem. Soc.*, **101**, 4481–4484.

Palmer III, A.G., Cavanagh, J., Wright, P.E. and Rance, M. (1991) *J. Magn. Reson.*, **93**, 151–170.

Peng, J.W., Thanabal, V. and Wagner, G. (1991) *J. Magn. Reson.*, **95**, 421–427.

Roder, H., Elöve, G.A. and Englander, S.W. (1988) *Nature*, **335**, 694–699.

Udgaonkar, J.B. and Baldwin, R.L. (1988) *Nature*, **335**, 700–704.

Van Doren, S.R., Kurochkin, A.V., Qi-Zhuang, Y., Johnson, L.L., Hupe, D.J. and Zuiderweg, E.R.P. (1993) *Biochemistry*, **32**, 13109–13122.

Wagner, G. (1993) *J. Biomol. NMR*, **3**, 375–385.

Wang, A.C. and Bax, A. (1993) *J. Biomol. NMR*, **3**, 715–720.

Zuiderweg, E.R.P. and Fesik, S.W. (1989) *Biochemistry*, **28**, 2387–2391.